NIGERIAN JOURNAL OF MATERIALS SCIENCE AND ENGINEERING
NJMSE
ISSN 214-453-2

GEOLOGICAL AND CHEMICAL CHARACTERIZATION OF AMETHYST MINERALIZATION IN DUTSEN BAKURA HILL, KADUNA STATE, NORTHCENTRAL NIGERIA

R. A. SOLOMON, * A. A. IBRAHIM, ** AND S. S. MAGAJI ***
Nuhu Bamalli Polytechnic, P.M.B. 1061, Zaria.
Department of Geology, Ahmadu Bello University, Zaria
[iyarose63@yahoo.com]

ABSTRACT
Dutsen Bakura hill amethyst mineralization is located within a sheared granitic gneiss in the Pan-African basement complex of northcentral Nigeria. The zone of mineralization is within a shear zone that trend NE-SW consistent with Pan-African structural trend. Mineralization consists of bands of milky quartz and amethyst, apparently formed from two stage sequence of silicification. Major, trace and rare earth element (REE) distribution patterns are used to distinguished host rock and mineralization characteristic. SiO_2 content ranges generally between 76.77 – 79.25 wt % ; Al_2O_3 content ranges between 11.61 – 11.85 wt %; Fe_2O_3(T) content ranges between 1.49 – 2.26 wt %; Na_2O content ranges between 2.91 - 4.99 wt % in the granite gneiss. The sheared granite gneiss has SiO_2 content ranging between 82.09 w % - 99.21 wt %; Al_2O_3 content ranging between 7.42 - 10.34 wt % which is slightly lower than that of the granite gneiss; Fe_2O_3 (T) content ranges between 0.67 – 3.90 wt %; Na_2O content ranges between 0.01 - 0.02 wt %. Major element content distribution within the mineralised zone is as follows: The SiO_2 content in the amethyst ranges from 98.95 - 100 wt %; Al_2O_3 ranges between 0.06 – 0.18 wt %; Fe_2O_3 (T) ranges between 0.63 – 0.67 wt %; Na_2O content ranges between 0.01 -0.02. However, SiO_2 in the milky quartz ranges from 97.43 to 99.22 wt%; Al_2O_3 content ranges between 0.05 – 0.22 wt %; Fe_2O_3 (T) content ranges between 0.56 – 0.66 wt %; Na_2O content ranges between 0.01 -0.02 wt %. This paper reports the geological and chemical characteristics of amethyst mineralization of Dutsen Bakura hill with the general view of chemically characterizing Nigerian amethyst.

Keywords: *Amethyst, Geology, Mineralization, Characterization, Shear Zone, Silicification*

1.0 INTRODUCTION

Amethyst is the violet variety of quartz that is commonly used as a semi-precious stone and is found in a number of locations in the basement complex rocks of the Zaria region of north-western Nigeria. The amethyst mineralization appears to be associated with fault structures as observed in the Dutsen Bakura hill area (Fig 1). The Dutsen Bakura hill amethyst occurs as a vein that developed in a sheared zone (about 1 Km along) within granite gneiss. This paper reports the geological and chemical characteristics of amethyst mineralization of Dutsen Bakura hill with the general view of chemically characterizing Nigerian amethyst.

2.0 CHEMISTRY OF AMETHYST

The violet colour of amethyst has been attributed to the following: i) presence of trace elements as inclusions in the quartz matrix ii) as substitutes for silicon in interstitial positions in the quartz crystal lattice, and iii) exposure of quartz to natural ionizing irradiation (Lehmann and Moore, 1966; Lehmann, 1971; Cohen and Makar, 1982 and Partlow and Cohen, 1986). Aluminum and iron are the trace elements usually assigned as substitutes for silicon in quartz lattice. If Al^{3+} or Fe^{3+} replace Si^{4+} in the centre of a SiO_4 tetrahedron (designated as Al_{Si}^{3+} or Fe_{Si}^{3+}), the charge deficiency requires an interstitial positive monovalent ion in the vicinity to neutralize the electric charge. H^+, Li^+, and Na^+ are usually considered as charge compensators (Bahadur, 1993; 1994; 1995; 2003 and 2006; Guzzo *et al.*, 1997; Bachheimer, 1998).

Hassan and Cohen (1974) proposed the colour in amethyst to be specifically attributed to the Fe^{4+} ion in an interstitial site, with absorption bands at 3.54, 2.28, and 1.30 eV (). However, formation of amethyst requires both the presence of substitutional $A1^{3+}$ and suppression of the A_1, A_2, and A_3 colour bands, which it creates (Partlow and Cohen, 1986). Cohen, (1985) proposed that amethyst formed in the following manner accounts for the above stated properties: $A1 - O^- \rightarrow A1 - O^o + e^-$ (formation of trapped holes centre A_l, A_2, and A_3 by ionizing radiation). $Na^+ + e^- \rightarrow Na^o$ (interstitial alkali ion traps electron centre). $Fe_i^{3+} \rightarrow Fe_i^{4+} + e^-$ (quenching of trapped hole on aluminium by electron furnished by $A1 - O^o + e^- \rightarrow A1 - O^-$ radiation induced oxidation of interstitial ferric iron). Lattice distortion may also contribute to the formation of colour in amethyst. This is expected if an iron atom replaces a silicon atom. The ionic radius of the iron is large enough to cause distortions in the tetrahedral configuration of the quartz lattice. The iron also has an electronic configuration very different from the one of silicon. Its outer electrons are 3d64s2, whereas the aluminum outer electrons are 3s22p1 (like the silicon radius, 3s22p2). This difference causes additional distortions in the lattice in the vicinity of an iron atom because the tetrahedral configuration causes crystal field splitting of the 3d-orbitals of iron into two groups, with a lower energy splitting difference. Adekeye and Cohen (1986) demonstrated that the interstitial ferric ion is located in specific channels in the quartz structure, particularly within the $(10\bar{1}1)$ rhombohedral plane.

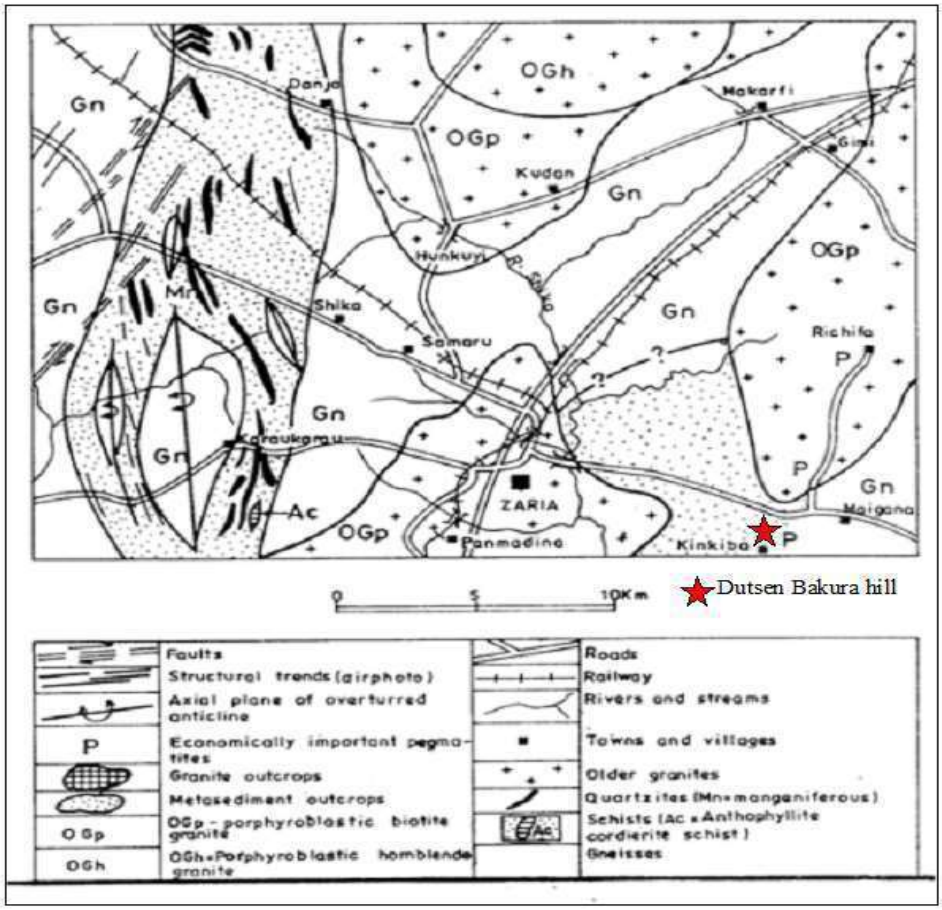

Fig 1: Geologic map of sheet 102 (Zaria) as modified after Garba (2009).

3.0 MATERIALS AND METHODS

The materials used and methods adopted in this research work are: fieldwork using topographical map, geological compass, Global Positioning System (GPS) and laboratory analysis that includes thin section, petrography, major and trace element geochemistry.

3.1 Fieldwork

Geological field mapping on a scale of 1:10,000 was undertaken and a total of thirty-six (36) representive samples were collected along carefully selected traverse lines from all representative rock units in Dutsen Bakura hill. Sample of amethyst from amethyst vein were collected at 10m interval to allow for the determination of elemental variations.

3.2 Laboratory Work and Analytical Techniques

Thin sections were produced in the Department of Geology, Ahmadu Bello University, Zaria Laboratories using 30 microns Conventional thin section procedure. Petrographic analyses were carried out using Optical and photomicrography microscope in the same Laboratories. Thirteen (13) samples were selected for whole rock geochemical analysis. The samples were broken into smaller chips and handpicked to avoid contamination at the laboratories of the Department of Geology, Ahmadu Bello University, Zaria and shpped to the Activation Laboratories Limited (ACTLABS), Ancaster, Ontario, Canada. Where major, trace and rare element analyses were carried out using Lithium metaborate/tetraborate fusion, Inductively Coupled Plasma emission spectrometry (ICP) and Inductively Coupled Plasma emission mass spectrometry analysis (ICP/MS).

4.0 RESULTS

4.1 Geology and Petrology

The predominant rock unit in the study area is a granite gneiss that was later sheared in some places to host the mineralized amethyst vein (Fig 2 A). Minor lithological units mapped are quartz veins in which the amethyst mineralization occurs and aplite dykes. Structures such as joints, faults, folds and foliation were observed in the study area. Alluvium, laterites and soil occur as superficial cover.

Granite gneiss

Granite gneiss constitutes about 80% of the study area. The rock is poorly exposed in the study area except in some localities such as: Ungwan Rimi, Sabon Kaura, Dutsen Bakura, Gidan Rano and Ungwan Turaki (Fig 2 B). The texture ranges from fine-medium to course-grained, granular and slightly foliated. The foliation is broadly oriented north-south and marked by a sub-parallel alignment of elongate and closely packed feldspar phenocrysts and a corresponding preferred orientation of biotite (Fig 2 C). The granite gneiss consists of about 30% quartz, 10% orthoclase, 25% plagioclase, 10% microcline and 25% biotite (Fig 2 D, E).

Few aplite dykes occurs in the granite gneiss. It is lightly greyish, is composed dominantly of plagioclase feldspar, quartz and mica minerals. It is uniformly fine-grained, less than 20 cm wide with characteristic granular texture.

Sheared granite gneiss

The sheared granite gneiss is a dense fine grained greyish and strongly foliated rock characterized by intense micro folding of milky quartz. Contact between the sheared granite gneiss and mineralized vein is sharp. The mineral constituents present are the same with those of the granite gneiss with a pronounced linear fabric defined by elongated minerals (Fig 2 F).

Quartz veins

Quartz veins occur as fracture and joint fillings in the granite gneiss and sheared granite gneiss. Milky quartz is the major mineral forming factures and joints fillings in the study area. Most of these veins are crystalline and are fine to medium-grained in nature. The quartz veins range in size from few mm of minutes thread in the sheared granite gneiss to over 10 cm in the granites gneiss (Fig 2 F). . The quartz veins exhibit irregularity in size and this causes them to widen and / or thin out along strike or longer axis. Some of the veins intersect each other within the sheared gneiss. The strike directions for crosscutting veins in the granite gneiss and sheared granite gneiss plotted show a general NNE-SSW dominant trend consistent with the Pan-African trend (Fig 2 G).

Mineralogy of the Amethyst Vein

The amethyst vein (mineralized zone) contains almost entirely quartz crystals with width of about 4.3 to 7.3m. The Dutsen Bakura hill amethyst vein shows variations in quartz colour. Quartz appears in different shades of purple and milky colour as druses (in vug) that are crystalline crust that only show the pointed terminations. In few of them, only the tips of the crystals are deeply coloured, the remainder grading into milky quartz (Fig 2 H).

4.2 Whole Rock Geochemistry

Analytical data expressed as major oxides and trace elements, Rare earth element (REE), along with the calculated petrochemical parameters and ratios are presented in Table 1, 2 and 3. The chemical data obtained from the analyzed rock samples were processed using a GCDKit (Geochemical Data Tool Kit) computer software. A chondrite discrimination diagram was used to plot the Chondrite-normalized REE patterns Fig 3.

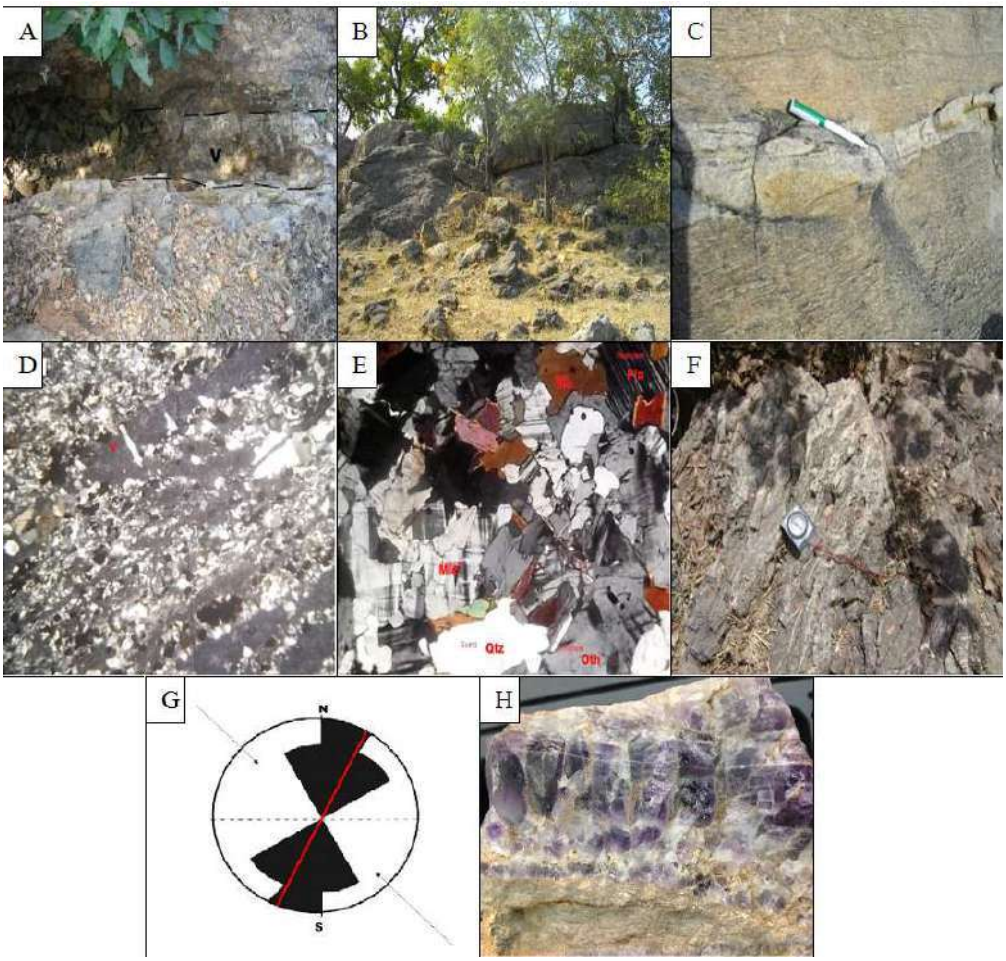

Fig 2: Pictures showing geological and mineralogical characteristic of Dusten Bakura hill

Major and trace elements

The major element compositions of the granite gneiss, the sheared granite gneiss, milky quartz and amethyst veins as presented in Table 1 show that the bulk chemical compositions of the results are variable to a considerable extent. The most notable characteristic of the grante gneiss is that it has SiO_2 content ranging between 76.77 to 79.25wt % (generally >70 wt %) and Al_2O_3 content ranges between 11.61 to 11.85 wt % (<11 wt %). Whereas the sheared granite gneiss has SiO_2 content ranging between 82w% to 84 wt %), which is higher than that of the granite gneiss and a Al_2O_3 content ranging between 7wt%-10 wt % which is slightly lower than that of the granite gneiss. The SiO_2 content of the amethyst range from 98.95 to 100.1wt %, while that of the milky quartz range from 94.43 to 99.22 wt%. Na_2O and K_2O values are below detection limit in both the amethyst and milky quartz.

The total iron contents expressed as Fe_2O_3 for granite gneiss range from 1.49-2.26 wt %, whereas the sheared granite gneiss has higher Fe_2O_3 content of 3.9wt %. However, the milky quartz and amethyst have less than 1 wt% Fe_2O_3. There is no exceptional enrichment in iron either in the amethyst or milky quartz. The total iron content in quartz is known to be temperature dependent and its concentration increases with temperature (Holden, 1925).

The TiO_2 concentrations in the amethyst and milky quartz samples are between 0.001 and 1.002wt%. However, five samples from the amethyst and milky quartz have TiO_2 values of 0.001wt% indicating a low content of Ti in the samples. The CaO and MgO concentrations in the granite gneiss and sheared granite gneiss are less than 1 wt% each, except in sample BK 21/8 which has CaO content of 1.15 wt% and MgO content of 0.12 wt%. The granite gneiss is enriched in the following lithophile elements: Ba, Rb, Th, Zn, U, Y, Hf, and Tm when compared to the sheared granite gneiss but depleted in Cs, Ba, Sr, Ta, W, Pb, and Tl (Table 2, 3).

Chondrite normalized pattern of the rare earth elements show that the granite gneiss and the sheared granite gneiss have high light rare earth elements (LREE) abundances (∑LREE 157.04) and slightly fractionated pattern (La_N/Yb_N=1.7-9.1), as well as a marked negative Eu and a weakly negative Ce anomalies (Fig 3). The granite gneiss and sheared granite gneiss have similar negative anomaly though it is stronger in the granite gneiss (Eu/Eu*=0.3) than it is in the sheared granite gneiss (Eu/Eu*=0.3-0.6). There is a general slight depletion of the heavy rare earth elements (HREE) in sheared gneiss. The chondrite normalized patterns of the REE for sheared granite gneiss are parallel to those of the granite gneiss but at slightly lower absolute abundances. However, the REE pattern of the amethyst is parallel to that of the milky quartz but the patterns are slightly irregular probably as a result of the quartz having a closed system or a characteristic tetrad effect.

5.0 CONCLUSION AND RECOMMENDATION

It is concluded that the amethyst mineralization in Dusten Bakura hill, Kaduna State, north central Nigeria which occur within the Pan-African basement complex of north central Nigeria may probably be due to crystallization of residual solutions in fissures and cavities of the basement rocks under low temperature and pressure conditions.

Due to its attractive appearance and hardness amethyst is used extensively for decorative purposes. It is used for jewellery; it is used in the manufacture of ornaments, crystal balls, table-tops, book-ends, vases, mosaics, statues; as well as for indoor and outdoor decorative purposes such as fireplace mantles and building facing stone.

Production of this amethyst deposit in the study area is mostly carried out by informal small scale miners who exploit these mineral through open cast mining. However, the amethyst mineralization within the Pan-African basement complex of northcentral Nigeria could support local industries. As such, it is recommended that such an industry be established to increase the socio-economic development of the area.

Table 1: Major element composition in rocks from Dutsen Bakura hill (values in wt %).

Rock type /Sample No/ Oxides	Granite Gneiss			Sheared Granite Gneiss				Milky Quartz			Amethyst		
	BK1/15	BK1/14	BK21/8	BK2/14	BK2/15	BK21/6	BK3/15	BK17/14	BK13/14	BK23/14	BK15/14	BK51/14	BK3/14
SiO_2	76.77	76.93	79.25	84.32	82.09	83.4	99.21	97.43	98.43	99.22	100.1	98.95	99.74
Al_2O_3	11.61	11.69	11.85	7.42	10.34	8.66	0.61	0.21	0.22	0.05	0.18	0.16	0.06
Fe_2O_3(T)	1.83	2.26	1.49	2.47	1.82	3.9	0.67	0.6	0.66	0.56	0.63	0.65	0.67
MnO	0.019	0.055	0.032	0.011	0.004	0.011	0.01	0.006	0.006	0.006	0.006	0.006	0.007
MgO	0.07	0.06	0.12	0.12	0.01	0.21	0.02	0.01	0.01	0.01	0.01	0.01	0.01
CaO	0.61	0.47	1.15	0.05	0.03	0.05	0.03	0.02	0.02	0.02	0.02	0.02	0.02
Na_2O	2.91	3.92	4.99	0.01	0.02	0.02	0.02	0.02	0.01	0.01	0.02	0.01	0.01
K_2O	5.65	4.29	0.79	0.33	0.06	0.67	0.02	0.01	0.01	0.01	0.01	0.01	0.01
TiO_2	0.102	0.097	0.108	0.84	0.104	0.847	0.015	0.001	0.001	0.002	0.001	0.001	0.001
P_2O_5	0.01	0.01	0.01	0.05	0.06	0.06	0.01	0.01	0.01	0.01	0.01	0.01	0.01
LOI	0.36	0.22	0.27	2.75	4.19	2.97	0.28	-0.02	0.03	0.06	-0.03	-0.04	0
Total	99.93	100	100.1	98.36	98.72	100.8	100.9	98.3	99.38	99.92	101	99.75	100.5

Table 2: Trace-Element Abundances in rocks from Dutsen Bakura Hill (values in ppm).

Rock type /Sample No/ Oxides	Granite Gneiss			Sheared Granite Gneiss				Milky Quartz			Amethyst		
	BK1/15	BK1/14	BK21/8	BK2/14	BK2/15	BK21/6	BK3/15	BK17/14	BK13/14	BK23/14	BK15/14	BK51/14	BK3/15
Sc	3	3	7	9	3	11	1	1	1	1	1	1	1
Be	3	4	7	2	1	2	1	3	3	1	5	4	1
V	5	12	8	76	9	95	7	5	5	5	5	5	7
Ba	377	382	79	70	22	178	30	7	8	3	7	4	30
Sr	28	27	46	52	35	93	7	2	2	2	2	2	7
Y	163	144	184	24	104	34	3	2	2	2	2	2	3
Zr	574	467	405	246	581	251	4	6	4	4	4	4	4
Cr	20	20	20	290	20	290	20	20	20	20	20	20	20
Cu	10	100	10	10	100	10	10	10	10	10	10	10	10
Zn	100	220	110	30	90	30	30	30	30	30	30	30	30
Ga	21	23	21	22	19	18	2	4	3	1	4	4	2
Ge	3	3	3	1	2	1	1	1	1	1	1	1	1
Rb	274	228	31	24	5	58	2	2	2	2	2	2	2
Nb	67	46	53	21	44	23	1	1	1	1	1	1	1
Ag	3.3	3.3	2.4	1.4	4.1	1.5	0.5	0.5	0.5	0.5	0.5	0.5	0.5
Sn	13	10	9	13	8	17	1	1	1	1	1	1	1
Sb	0.6	0.5	0.6	0.6	0.5	0.6	0.5	0.5	0.5	0.5	0.5	0.5	0.5
Cs	2.2	1.3	0.5	1.3	0.5	2.3	0.5	0.5	0.5	0.5	0.5	0.5	0.5
Hf	25.8	19.4	16.7	6.2	25.1	6.3	0.2	0.2	0.2	0.2	0.2	0.2	0.2
Ta	5	3.6	4.9	0.8	3.6	0.8	0.1	0.1	0.1	0.1	0.1	0.1	0.1
W	1.99	3.61	1.18	12.1	1.61	8.21	0.86	1.88	0.57	0.44	5.59	0.47	0.86
Tl	1	0.8	0.2	0.1	0.1	0.3	0.1	0.1	0.1	0.1	0.1	0.1	0.1
Pb	35	57	36	70	27	66	6	5	5	5	5	5	6
Bi	0.4	0.4	0.4	1.6	0.4	0.9	0.4	0.4	0.4	0.4	0.4	0.4	0.4
Th	25.8	21.3	68.2	8.9	14.5	8.7	0.3	0.7	0.1	0.1	0.1	0.1	0.3
U	13.6	9.5	9.8	5.4	6.2	10.6	0.6	0.1	0.1	0.1	0.1	0.1	0.6

Table 3: REE-Element data in rocks from Dutsen Bakura Hill (values in ppm).

Rock type /Sample No/ Oxides	Granite Gneiss			Sheared Granite Gneiss				Milky Quartz			Amethyst		
	BK1/15	BK1/14	BK21/8	BK2/14	BK2/15	BK21/6	BK3/15	BK17/4	BK13/14	BK23/14	BK15/14	BK51/14	BK3/14
La	37.1	58.6	64.4	59.6	64.5	54.5	8.9	1	0.4	0.3	0.3	0.2	0.3
Ce	72.5	105	94.9	97.5	120	65.9	6.3	1.3	0.5	0.5	0.3	1.1	0.4
Pr	8.84	12.3	13.6	13.4	14.4	11.6	1.95	0.18	0.08	0.07	0.06	0.06	0.08
Nd	30.5	45.9	47.3	45.7	52.7	39.1	6.3	0.6	0.2	0.2	0.1	0.2	0.3
Sm	8.1	11.2	12.6	9.7	12.3	7.7	1.3	0.1	0.1	0.1	0.1	0.1	0.1
Eu	0.7	0.98	1.11	1.5	1.17	1.29	0.16	0.05	0.05	0.05	0.05	0.05	0.05
Gd	9.3	13.4	16.2	7	11.9	6.2	0.9	0.2	0.1	0.1	0.1	0.1	0.1
Tb	2.2	2.9	3.6	1.2	2.5	1	0.2	0.1	0.1	0.1	0.1	0.1	0.1
Dy	15.9	20.8	26.3	6.3	16.8	6.4	0.7	0.2	0.1	0.1	0.1	0.1	0.1
Ho	3.5	4.7	5.9	1.2	3.8	1.4	0.1	0.1	0.1	0.1	0.1	0.1	0.1
Er	11.4	14.6	19.1	3.4	12.2	4.3	0.3	0.1	0.1	0.1	0.1	0.1	0.1
Tm	1.99	2.49	3.24	0.58	2.07	0.71	0.05	0.05	0.05	0.05	0.05	0.05	0.05
Yb	14.2	18.2	22.9	4.2	14.9	5.1	0.3	0.2	0.1	0.1	0.1	0.1	0.1
Lu	2.45	3.16	3.91	0.62	2.46	0.85	0.05	0.04	0.04	0.04	0.04	0.04	0.04
Eu/Eu*	0.25	0.25	0.24	0.56	0.3	0.57	NA	1.09	1.54	1.54	1.54	1.54	1.54
LaN/YbN	1.74	2.15	1.87	9.46	2.89	7.12	19.78	3.33	2.67	2	2	1.33	2
LaN/SmN	2.82	3.22	3.14	3.78	3.23	4.35	4.21	6.15	2.46	1.85	1.85	1.23	1.85
CeN/YbN	1.3	1.47	1.05	5.9	2.05	3.29	5.34	1.65	1.27	1.27	0.76	2.8	1.02
CeN/SmN	2.1	2.2	1.77	2.36	2.29	2.01	1.14	3.05	1.17	1.17	0.7	2.58	0.94
EuN/YbN	0.14	0.15	0.14	1.02	0.22	0.72	NA	0.71	1.43	1.43	1.43	1.43	1.43
Σ-REE	218.68	314.23	335.06	251.9	331.7	206.05	26.95	4.22	2.02	1.91	1.6	2.4	1.92

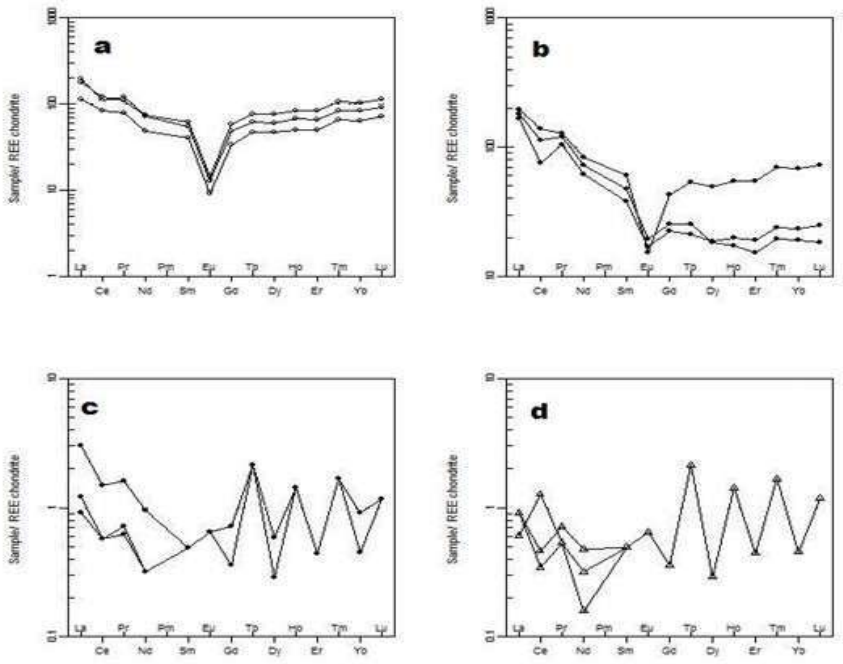

Fig 3: Chondrite-normalized REE patterns of the granite gneiss (a), sheared gneiss (b), milky quartz (c) and amethyst (d) from Dutsen Bakura hill. Normalizing values are those of Nakamura, (1974).

REFERENCES

Adekeye, J. I. D. and Cohen, A. J. (1986). Correlation of Fe^{4+} optical anisotropy, Brazil twinning and channels in the basal plane of amethyst quartz. *Applied Geochemistry* **1,** 152-160.

Bachheimer, J. P. (1998). An investigation into hydrogen stability in synthetic, natural and air-swept synthetic quartz in air temperatures up to 1100 °C. *Journal of Physics and Chemistry of Solid* **49** (5), 831-840

Bahadur, H. (1993). Hydroxyls defects and electrodiffusion (sweeping) in natural quartz crystals. *Journal of Applied Physics* **73**(11), 7790-7797.

Bahadur, H. (1994). Sweeping and irradiation effects on hydroxyls defects in crystalline natural quartz. *IEEE Transactions on Ultrasonics, Ferroelectrics, and Frequency Control* **41**(6), 820-833.

Bahadur, H. (1995). Sweeping investigations on as grown Al-Li+ and Al-OH centers in natural crystalline quartz. *IEEE Transactions on Ultrasonics, Ferroelectrics and Frequency Control* **42**(2), 153-158.

Bahadur, H. (2003). Radiation-induced modifications of point defects in quartz crystals and their application in radiation dosimetry. *Radiation Measurements*. **36**(1-6), 493-497.

Bahadur, H. (2006). Radiation induced modification of impurity-related point defects in crystalline quartz: a review. *Crystal Research and Technology.* **41**(7), 631-635.

Cohen, A. J. (1985). Amethyst colour in quartz, the result of radiation protection involving iron. *American Mineralogist* **70**, 1180-1185.

Cohen, A. J. and Makar, L. N. (1982). Models for colour centers in smoky quartz. *Physica Status Solidi.* **73**(2), 593-596

Garba, I. (2009). Zaria and its region. A Nigerian Savannah city and its environs. Occasion paper No 5.

Guzzo, P. L., Iwasaki, F. and Iwasaki, H. (1997). Al-related centers in relation to γ-irradiation. Response in natural quartz. *Physics and Chemistry of Minerals*. **24**(4), 254-263.

Hassan, F. and Cohen, A. J. (1974). Biaxial colour centres in amethyst quartz. *American Mineralogist* **59**, 709 -718.

Holden, F. H. (1925). The cause of colour in smoky quartz and amethyst Copyright © 1925 – 2004. *Mineralogical Society of America* All rights reserved.

Lehmann, G. (1971). Yellow colour centres in natural and synthetic quartz. Zeitschrift für Physik *B Condensed Matter* **13** (4), 297-306.

Lehmann, G. and Moore, W. J. (1966). Colour centre in amethyst quartz. *Science*. **152** (3725), 1061-1062.

Nakamura, N. (1974). Determination of REE, Ba, Fe, Mg, Na and K in carbonaceous and ordinary chondrites. *Acta Crystals* **38**, 757-775.

Partlow, D. P. and Cohen, A. J. (1986). Optical studies of biaxial Al-related colour centres in smoky quartz. *American Mineralogist* **71**, 589-598.